

Bi-dipole wave: optimum for attaining extreme regimes at matter-light colliders

Christoffer Olofsson and Arkady Gonoskov

Department of Physics, University of Gothenburg, SE-41296 Gothenburg, Sweden

(Dated: February 17, 2022)

The collision of accelerated electrons with high-intensity laser pulses provides a way for triggering and studying the processes of strong-field quantum electrodynamics by means of reaching high values of the χ parameter, the parameter that quantifies electron's acceleration in its rest frame. For a given electrons' energy ε and a given peak, cycle-averaged power P of the laser radiation the maximal value of χ depends on the way the radiation is focused to cause the acceleration. We determine and describe the optimal focusing geometry for reaching the highest possible value $\chi \approx 5.28 (\varepsilon/(1 \text{ GeV})) (P/(1 \text{ PW}))^{1/2} (\lambda/(1 \mu\text{m}))^{-1}$, where λ is the laser wavelength. We propose an experimental setup that exploits the bi-dipole wave and assess this setup for the parameters relevant to current and upcoming experimental capabilities.

I. INTRODUCTION

The progress in technologies of high-intensity lasers and charged particle accelerators conceived fundamental opportunities to study extreme regimes of radiation reaction (RR) and other effects of strong-field quantum electrodynamics (SFQED) (see [1, 2] and references therein). The technical capabilities of laser facilities can be characterized by the total, peak, cycle-averaged power P that ranges from 1 PW to 20 PW at the current/upcoming large-scale laser facilities and is anticipated to reach ~ 100 PW scale at the future facilities [3–7]. The field strength of focused laser radiation can be characterized by the Lorentz invariant, dimensionless parameter a_0 being the field amplitude in the units of $mc\omega/|e|$, where ω is the laser frequency, c is the speed of light, m and e are the electron mass and charge, respectively. The effect of strong fields on an electron is characterized by the dimensionless acceleration in its rest frame χ , which can be boosted by the gamma factor γ of the electron in case of head-on collision with a counter-propagating laser pulse. The value of χ is normalized so that $\chi \gtrsim 1$ designates quantum regime of RR, whereas $\chi \gtrsim 1600$ demarcates qualitatively unexplored regimes characterized by the conjectured breakdown of perturbative nonlinear QED [8–10].

Conceptually, two main experimental configurations can be outlined: laser-beam colliders and laser-target colliders. In the former case electromagnetic fields of focused laser radiation act on externally accelerated counter-propagating electrons, whereas in the latter case the same laser fields also accelerate electrons being taken from a target. In the '90s the collision of 46.6-GeV electrons with focused laser pulses with peak intensity of $1.3 \times 10^{18} \text{ W/cm}^2$ was used to observe multiphoton Compton scattering [11] and multiphoton Breit-Wheeler pair creation [12]. Revisiting this experimental configuration with extended experimental program is a matter of several initiatives, including the E320 collaboration at FACET-II [13] and the LUXE (Light Und XFEL Experiment) collaboration at the European XFEL [14]. Another experimental alternative is based on the replace-

ment of conventional acceleration by laser wake-field acceleration (LWFA). This has been recently used to observe RR in extreme regimes [15, 16]. Although reaching high values of a_0 for a given power P is essential for laser-beam colliders, the use of more advanced strategies than tight focusing is not broadly discussed in the literature [17]. The situation is different for the laser-target colliders, for which reaching strong fields is the main key. The possibility of creating the strongest field by the dipole wave [18, 19] using multiple colliding laser pulses (MCLP) [20] has been recognized to enable many possibilities, ranging from particle trapping and photon generation [21–23] to the creation of sustained electromagnetic cascades and extreme electron-positron plasma states [24, 25].

In this paper we point out that reaching the highest possible value of χ is not the same as creating the strongest field and thus the dipole wave is not the optimal geometry. We determine the optimal geometry for reaching the highest possible value of χ for a given power P and provide characteristics that are essential for the future experimental efforts within the concept of laser-beam collider. The optimal geometry, being called bi-dipole wave, can provide more than 3 times higher values of χ than that provided by $f/2$ focusing, which means that the same values of χ can be reached using electrons of factor 3 lower energy or the laser facility of factor 9 lower total power. We estimate that $\chi = 1600$ can be reached by 200 GeV electron accelerator combined with a 2.3 PW laser facility or by 20 PW laser facility combined with a 70 GeV electron accelerator.

II. MAXIMIZATION PROBLEM

In case the energy of electrons is high enough ($\gamma \gg a_0 \gg 1$), the electromagnetic fields do not deflect them significantly while they pass through the few-cycle laser pulse and the value of χ is predominantly determined by the product of the gamma factor γ and the acceleration

in the direction perpendicular to the direction of motion:

$$\chi = \gamma \frac{\sqrt{(\mathbf{E} + (\mathbf{v}/c) \times \mathbf{B})^2 - (\mathbf{E} \cdot \mathbf{v}/c)^2}}{E_{\text{cr}}}, \quad (1)$$

where \mathbf{v} is the electron velocity, \mathbf{E} and \mathbf{B} are the electric and magnetic field created by the laser at the location of the electron. The critical field of QED is defined as $E_{\text{cr}} = m^2 c^3 / (e\hbar)$, where \hbar is the reduced Planck constant. In the context of reaching the highest possible values of χ the effect of the accelerator is quantified by the attainable energy $\varepsilon = mc^2\gamma$, whereas the capability of the laser is quantified by the total power P of laser radiation. To quantify the role of focusing we notice that in the focal region the intensity is proportional to P and inverse proportional to the focal area being proportional to λ^2 . Therefore the field strength scales as $\sim \lambda^{-1} P^{1/2}$ and $\chi \sim \gamma \lambda^{-1} P^{1/2}$. Thus, a focusing geometry can be quantified by a single dimensionless parameter σ that determines the peak value of χ (we assume that $\gamma \gg 1$ and thus $|\mathbf{v}| \approx c$):

$$\chi = \sigma \left(\frac{\varepsilon}{1 \text{ GeV}} \right) \left(\frac{P}{1 \text{ PW}} \right)^{1/2} \left(\frac{\lambda}{1 \mu\text{m}} \right)^{-1}. \quad (2)$$

The problem of finding the focusing geometry with the largest possible value of σ belongs to the class of optimization problems in optics. In 1986, using multipole expansion, Bassett showed that the dipole component provides the highest possible energy density for a given value of P and this optimal component also provides the strongest field strength $a_0 \approx 780 (P/(1 \text{ PW}))^{1/2}$ [18]. The authors of Ref. [19] carried out further analysis of the dipole wave and developed the theory of the so-called dipole pulse that is an exact solution constrained in all four dimensions.

To determine the optimal geometry for reaching the highest possible acceleration for an ultra-relativistic particle, we assume that the maximal value of χ is achieved at the origin of spherical coordinate system (r, θ, ϕ) with the electric field pointing towards $\theta = 0$. Assuming that the incoming wave is monochromatic, the field of the optimal geometry can be expressed as the real part of $\exp(-i\omega t)$ multiplied by some complex field $(\mathbf{E}^x, \mathbf{B}^x)$, which in turn can be expressed in the basis of electric $(\mathbf{E}^E, \mathbf{B}^E)$ and magnetic $(\mathbf{E}^B, \mathbf{B}^B)$ multipoles (exact so-

lutions of Maxwells' equations) given by [26]:

$$\begin{aligned} E_r^E &= \frac{l(l+1)}{r} j_l(kr) Y_l^m(\theta, \phi), \\ E_\theta^E &= \frac{1}{r} \frac{\partial}{\partial r} (r j_l(kr)) \frac{\partial}{\partial \theta} Y_l^m(\theta, \phi), \\ E_\phi^E &= \frac{im}{\sin \theta} \frac{1}{r} \frac{\partial}{\partial r} (r j_l(kr)) Y_l^m(\theta, \phi), \\ H_r^E &= 0, \\ H_\theta^E &= \frac{km}{\sin \theta} j_l(kr) Y_l^m(\theta, \phi), \\ H_\phi^E &= ik j_l(kr) \frac{\partial}{\partial \theta} (Y_l^m(\theta, \phi)), \\ \mathbf{E}^B &= -\mathbf{B}^E, \quad \mathbf{B}^B = \mathbf{E}^E, \end{aligned} \quad (3)$$

where $l = 1, 2, 3, \dots$, $m = -l, -l+1, \dots, l$, $k = \omega/c$, $j_l(kr)$ and $Y_l^m(\theta, \phi)$ are spherical Bessel functions and spherical harmonics, respectively. The subscripts denote vector components along the unit vectors that can be expressed in terms of components of Cartesian coordinate system:

$$\begin{aligned} \hat{\mathbf{r}} &= \sin \theta \cos \phi \hat{\mathbf{x}} + \sin \theta \sin \phi \hat{\mathbf{y}} + \cos \theta \hat{\mathbf{z}}, \\ \hat{\theta} &= \cos \theta \cos \phi \hat{\mathbf{x}} + \cos \theta \sin \phi \hat{\mathbf{y}} - \sin \theta \hat{\mathbf{z}}, \\ \hat{\phi} &= -\sin \phi \hat{\mathbf{x}} + \cos \phi \hat{\mathbf{y}}. \end{aligned} \quad (4)$$

Bassett showed that in terms of incoming power the multipolar components are additive, i.e. for any their combination the incoming power is the sum of incoming powers of the components [18]. Following Bassett we consider the limit $r \rightarrow 0$ and notice that only six components contribute to the field at the origin of the coordinate system (\mathbf{E} is formed by $\mathbf{E}_{l,m}^E$ and \mathbf{B} is formed by $\mathbf{B}_{l,m}^B$, in both cases $l = 1, m = -1, 0, 1$):

$$\mathbf{E}_{1,-1}^E = \mathbf{B}_{1,-1}^B = k \left(\frac{1}{6\pi} \right)^{1/2} (\hat{\mathbf{x}} - i\hat{\mathbf{y}}), \quad (5)$$

$$\mathbf{E}_{1,0}^E = \mathbf{B}_{1,0}^B = k \left(\frac{1}{3\pi} \right)^{1/2} \hat{\mathbf{z}}, \quad (6)$$

$$\mathbf{E}_{1,1}^E = \mathbf{B}_{1,1}^B = -k \left(\frac{1}{6\pi} \right)^{1/2} (\hat{\mathbf{x}} + i\hat{\mathbf{y}}). \quad (7)$$

According to our assumption \mathbf{E}^x is pointing towards $\theta = 0$ (i.e. towards $\hat{\mathbf{z}}$) and thus it is formed exclusively by the component $\mathbf{E}_{1,0}^E$. Without loss of generality we can assume that the coordinate system is oriented so that $\mathbf{B}^x(r=0)$ is laying in the xz plane and thus it is formed by a combination of $\mathbf{B}_{1,0}^B$ and $2^{1/2} (\mathbf{B}_{1,-1}^B - \mathbf{B}_{1,1}^B)$ components (the factor is chosen to provide synchronous peaking). The components $\mathbf{E}_{1,0}^E$ and $\mathbf{B}_{1,0}^B$ correspond to the electric and magnetic dipole waves with symmetry axis along $\hat{\mathbf{z}}$, whereas $2^{1/2} (\mathbf{B}_{1,-1}^B - \mathbf{B}_{1,1}^B)$ corresponds the magnetic dipole wave with symmetry axis along $\hat{\mathbf{x}}$. Given that the power of components is additive, we can describe all cases by splitting the total power P into three portions: aP is delivered by the electric dipole wave, whereas the portions bP and $(1-a-b)P$ are delivered

by the magnetic dipole waves with symmetry axes along $\hat{\mathbf{z}}$ and $\hat{\mathbf{x}}$, respectively; $0 \leq a, b \leq 1, a + b \leq 1$. The strength of components in relativistic units is given by

$$\mathbf{E} = a_d (P/(1 \text{ PW}))^{1/2} a^{1/2} \hat{\mathbf{z}}, \quad (8)$$

$$\mathbf{B} = a_d (P/(1 \text{ PW}))^{1/2} \left(b^{1/2} \hat{\mathbf{z}} + (1 - a - b)^{1/2} \hat{\mathbf{x}} \right), \quad (9)$$

where $a_d \approx 780$. If we were interested in the maximal energy density (i.e. $(E^2 + B^2)/(8\pi)$) all the possible cases were indifferent because the energy density is independent of a and b . Nevertheless, searching for the strongest possible acceleration yields one specific optimum. First we note that the maximal Lorentz force is achieved if the electron propagates along the y axis. In this case the absolute value of the Lorentz force and the χ value is proportional to

$$\chi \sim \left(\left(a^{1/2} + (1 - a - b)^{1/2} \right)^2 + b \right)^{1/2}. \quad (10)$$

Searching for the maximum of χ^2 we compute the derivative with respect to b :

$$\frac{\partial}{\partial b} \chi^2 = - \left(a^{1/2} + (1 - a - b)^{1/2} \right) (1 - a - b)^{-1/2} + 1. \quad (11)$$

Since the derivative is ≤ 0 for all values of a and b we conclude that the maximum is achieved at $b = 0$. Next, we compute $\partial \chi^2 / \partial a$ and determine that the maximum is achieved at $a = 1/2$.

As one can see the maximum corresponds to the equal destitution of energy between electric and magnetic dipole waves that have perpendicular axes. That is why we choose to call this geometry bi-dipole wave. The field strength is $|\mathbf{E}^x| = |\mathbf{B}^x| = a_d (P/(1 \text{ PW}))^{1/2} / \sqrt{2} \approx 550 (P/(1 \text{ PW}))^{1/2}$ (in relativistic units) and the value of σ is approximately 5.28.

III. BI-DIPOLE WAVE

In this section we describe the structure of the bi-dipole wave and quantify its characteristics in the context of possible experiments. For the sake of illustration we change the orientation of the bi-dipole wave so that its electric dipole axis is along y , see figure 1 (the magnetic axis is still pointing along x as previously). To within a constant factor the electric field vector in the far field region can be given by:

$$\mathbf{E}(r \rightarrow \infty) \sim r^{-1} (\mathbf{E}^e + \mathbf{E}^b), \quad (12)$$

$$\mathbf{E}^e = (\hat{\mathbf{y}} \times \mathbf{n}) \times \mathbf{n}, \quad (13)$$

$$\mathbf{E}^b = -(\hat{\mathbf{x}} \times \mathbf{n}), \quad (14)$$

where $\mathbf{n} = \mathbf{r}/r$, whereas \mathbf{E}^e and \mathbf{E}^b are proportional to the electric field vectors of the radiation forming electric and magnet dipole waves, respectively. The signs are

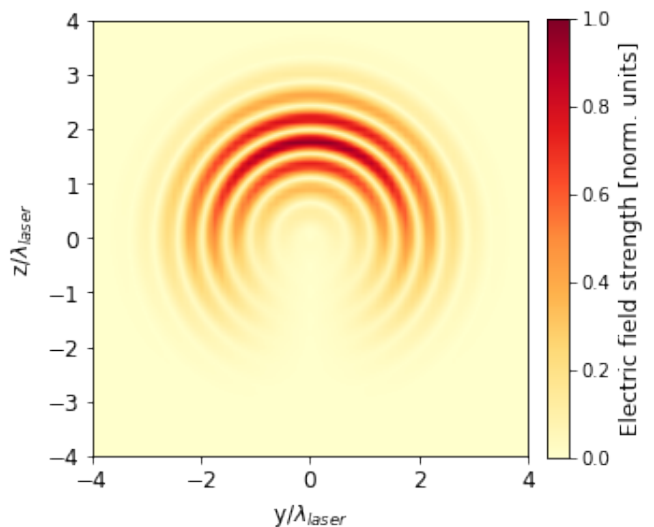


FIG. 1. Cross-section of the bi-dipole electric field strength in the yz -plane with a wavelength of $\lambda_{laser} = 0.8 \mu\text{m}$.

chosen so that the constructive summation of the electric and magnetic components is provided for a charge propagating towards the negative z direction.

Along each direction of incoming radiation the dipole waves are formed by linearly polarized, syn-phased waves and thus the bi-dipole wave is also formed by linearly polarized wave. Let us demonstrate that the intensity I of this wave is independent of θ . To do so we compute the intensity as a function of \mathbf{n} :

$$\mathbf{E}^e = n_x n_y \hat{\mathbf{x}} - (n_x^2 + n_z^2) \hat{\mathbf{y}} + n_z n_y \hat{\mathbf{z}},$$

$$\mathbf{E}^b = n_z \hat{\mathbf{y}} - n_y \hat{\mathbf{z}},$$

$$I \sim |\mathbf{E}^e + \mathbf{E}^b|^2 \sim n_x^2 n_y^2 + (n_x^2 + n_z^2 - n_z)^2 + n_y^2 (n_z - 1)^2, \quad (15)$$

where $n_z = \cos \theta$, $n_y = \sin \theta \sin \phi$, $n_x = \sin \theta \cos \phi$. Given that $\partial n_z / \partial \phi = 0$, $\partial n_y / \partial \phi = n_x$, $\partial n_x / \partial \phi = -n_y$, we compute

$$\frac{\partial I}{\partial \phi} \sim 2n_y n_x (1 - n_z^2 - n_y^2 - n_x^2) = 0. \quad (16)$$

Therefore the intensity of the incoming wave forming the bi-dipole wave is independent of ϕ .

If $\phi = 0$ is chosen, s.t. $\cos(\phi) = 1$ and $\sin(\phi) = 0$, then in Eq. (15) only the middle term remains and we have

$$I \sim (1 - \cos \theta)^2. \quad (17)$$

As we can see the radiation is arriving predominantly from the negative z hemisphere.

One possible way to form the bi-dipole wave is the reflection of an appropriate laser beam propagating towards negative z direction from a parabolic mirror. Let us compute the polarization and intensity distribution in such a beam. During reflection the electric field component along the normal \mathbf{N} to the mirror is reversed.

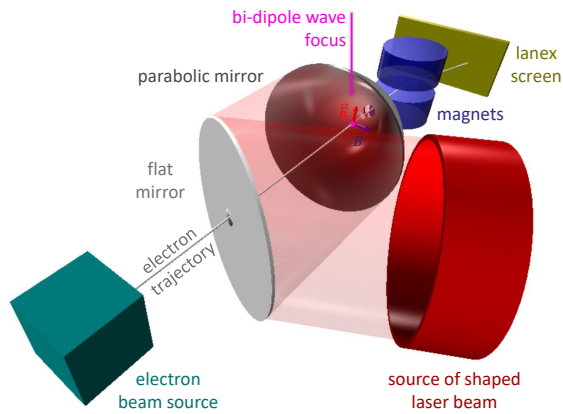


FIG. 2. Schematic representation of a possible experimental setup.

Thus, to within a factor the electric field before reflection is given by $\mathbf{E}^p = \mathbf{E} - 2(\mathbf{E} \cdot \mathbf{N})\mathbf{N}$, where the normal can be expressed as $\mathbf{N} = (\hat{\mathbf{z}} - \mathbf{n})/|\hat{\mathbf{z}} - \mathbf{n}|$. We note that $(\mathbf{E} \cdot \mathbf{N}) = (\mathbf{E} \cdot \hat{\mathbf{z}}) = n_y(n_z - 1)/|\hat{\mathbf{z}} - \mathbf{n}|$ and compute the x component of \mathbf{E}^p :

$$\begin{aligned} E_x^p &= n_x n_y - 2n_y(n_z - 1)(-n_x) \left(n_x^2 + n_y^2 + (n_z - 1)^2 \right)^{-1} \\ &= n_x n_y (n_z^2 + n_y^2 + n_x^2 - 1) \left(n_x^2 + n_y^2 + (n_z - 1)^2 \right)^{-1} \\ &= 0. \end{aligned} \quad (18)$$

As we can see the beam to be reflected has linear polarization exactly along y axis everywhere. Due to such a fortunate property, this configuration has been considered by Sheppard and Lerkin [27] as a notably practical option among all mixed dipole waves that yield the highest electromagnetic field density under focusing of a given power. As we demonstrated exactly this option also gives the highest value of χ and thus is optimal for the laser-based studies of SFQED. Finally, we compute and provide the intensity distribution in the optimal beam to be reflected by the parabolic mirror:

$$I^p(R) \sim \left(\left(\frac{R}{2L} \right)^2 + 1 \right)^{-4}, \quad (19)$$

where L is the distance to the mirror and R is the distance to the z axis in transverse plane.

IV. EXPERIMENTAL STRATEGIES

The next question that deserves consideration is how one can make use of the described field geometry for testing theoretical predictions in the domain of high χ values. One possible goal is retrieving the rate of electron emission as a function of photon energy at high values

of χ . The data that we can potentially obtain from experimental diagnostics includes the distribution of generated particles and photons as a function of energy and propagation direction. An obvious concern is related to the presence of a background signal due to particles and photons that are produced at low values of χ . In addition, if an electron emits several photons (even if all of them are emitted at high χ), we do not know the energies at each emission and thus cannot directly determine the sought-after rate. Thus, we set as a goal for further analysis finding strategies that ensures a notable part of *primary* high- χ particles/photons in certain part of parameters space. Hereafter *primary* electron means that the electron emitted exactly one high-energy photon (the remaining radiation losses are less than 1% of the initial energy), whereas *primary* photon means that the detected photon had been emitted by a primary electron. We call all other detected particles *secondary*. The ratio of primary particle/photon number to that of both secondary and primary particle/photon should be maximized. We note that this ratio, which we call signal-to-noise ratio, doesn't necessarily need to be close to unity. Even if the ratio is much smaller, we can still benchmark the predictions against the experimental results, whereas the larger values of the ratio favour the compared data to be more sensitive to the theoretical predictions. Large values of signal-to-noise ratio also favor Bayesian analysis.

Given that the strong field is localized to a region of μm size, it could be challenging to focus the electron beam so that the electrons propagate exclusively through this region. We thus assume that the electron beam is much larger than the strong-field region. In other words, we assume that the bi-dipole wave is formed in a uniform stream of electrons. We propose diagnostics by exploiting two ideas. First, we consider photons because they have longer average propagation distance to the occurrence of pair production than electrons propagate on average before the emission of the next high-energy photon. Thus they have a better chance to escape the strong-field region and contribute to the signal. Second, if an electron has a large χ value and emits a photon, this photon propagates almost along the current direction of electron propagation. This direction can deviate from the initial direction by an angle α that can be larger than anywhere beyond the strong-field region. Thus large deflection angles α correspond to photons that were generated predominantly in the strong-field region.

In fig. 3 we demonstrate the results of simulations using the described strategy for parameters that can be relevant to current and upcoming experimental capabilities. We consider a laser pulse that has a Gaussian profile with a duration of 5 cycles (FWHM for intensity); the laser wavelength is $1 \mu\text{m}$. In all simulations we exclude particles and photons with energy below 1% of the initial electron energy. In the first case, the total laser power is 1 PW and the energy of electron is 200 GeV. In this case we can see a notable number of photons pro-

duced at $\chi > 50$. The signal-to-noise ratio in the region of photon energies $\hbar\omega/(mc^2\gamma) > 0.5$ and $|\alpha| > 10^{-4}$ is $\sigma_{50} \approx 0.18$. In the third case, the total laser power is 10 PW and the energy of electron is 200 GeV. In this case we can see a notable number of photons produced at $\chi > 100$. The signal-to-noise ratio in the region of photon energies $\hbar\omega/(mc^2\gamma) > 0.5$ and $|\alpha| > 10^{-4}$ is $\sigma_{100} \approx 0.12$. In the second case, the total laser power is 10 PW and the energy of electron is 10 GeV. We can see that the strength of field suppresses the signal due to larger probability of secondary emissions and pair production. In this case we can take a different strategy and consider photons at low energy and small deflection

angles. The signal-to-noise ratio in the region of photon energies $0.01 < \hbar\omega/(mc^2\gamma) < 0.05$ and $|\alpha| < 2.5^{-3}$ is $\sigma_5 \approx 0.027$.

V. CONCLUSIONS

In this work we obtained focusing geometry of bi-dipole wave that provides the highest possible χ value for the given power of used radiation. We described the way of forming bi-dipole wave and proposed some strategies of using it for experimental studies of SFQED at high values of χ .

-
- [1] A. Di Piazza, C. Muller, K. Z. Hatsagortsyan, and C. H. Keitel, Extremely high-intensity laser interactions with fundamental quantum systems, *Rev. Mod. Phys.* **84**, 1177 (2012).
- [2] A. Gonoskov, T. G. Blackburn, M. Marklund, and S. S. Bulanov, Charged particle motion and radiation in strong electromagnetic fields (2021), [arXiv:2107.02161](https://arxiv.org/abs/2107.02161).
- [3] Eli white book, <https://eli-laser.eu/media/1019/eli-whitebook.pdf>, accessed: 2021-08-10.
- [4] Xcels white book, <https://xcels.ipfran.ru/img/XCELS-Project-english-version.pdf>, accessed: 2021-08-10.
- [5] Y. Kitagawa, H. Fujita, R. Kodama, H. Yoshida, S. Matsuo, T. Jitsuno, T. Kawasaki, H. Kitamura, T. Kanabe, S. Sakabe, K. Shigemori, N. Miyanaga, and Y. Izawa, Prepulse-free petawatt laser for a fast ignitor, *IEEE Journal of Quantum Electronics* **40**, 281 (2004).
- [6] J. Kawanaka, K. Tsubakimoto, H. Yoshida, K. Fujioka, Y. Fujimoto, S. Tokita, T. Jitsuno, and N. M. and, Conceptual design of sub-exa-watt system by using optical parametric chirped pulse amplification, *Journal of Physics: Conference Series* **688**, 012044 (2016).
- [7] C. N. Danson, C. Haefner, J. Bromage, T. Butcher, J.-C. F. Chanteloup, E. A. Chowdhury, A. Galvanauskas, L. A. Gizzi, J. Hein, D. I. Hillier, N. W. Hopps, Y. Kato, E. A. Khazanov, R. Kodama, G. Korn, R. Li, Y. Li, J. Limpert, J. Ma, C. H. Nam, D. Neely, D. Papadopoulos, R. R. Penman, L. Qian, J. J. Rocca, A. A. Shaykin, C. W. Siders, C. Spindloe, S. Szatmári, R. M. G. M. Trines, J. Zhu, P. Zhu, and J. D. Zuegel, Petawatt and exawatt class lasers worldwide, *High Power Laser Science and Engineering* **7**, 10.1017/hpl.2019.36 (2019).
- [8] V. Ritus, Radiative corrections in quantum electrodynamics with intense field and their analytical properties, *Annals of Physics* **69**, 555 (1972).
- [9] N. B. Narozhny, Expansion parameter of perturbation theory in intense-field quantum electrodynamics, *Physical Review D* **21**, 1176 (1980).
- [10] A. Fedotov, Conjecture of perturbative QED breakdown at $\alpha\chi^{2/3} \gtrsim 1$, *Journal of Physics: Conference Series* **826**, 012027 (2017).
- [11] C. Bula, K. T. McDonald, E. J. Prebys, C. Bamber, S. Boege, T. Kotsieroglou, A. C. Melissinos, D. D. Meyerhofer, W. Ragg, D. L. Burke, R. C. Field, G. Horton-Smith, A. C. Odian, J. E. Spencer, D. Walz, S. C. Berridge, W. M. Bugg, K. Shmakov, and A. W. Weidemann, Observation of nonlinear effects in Compton scattering, *Physical Review Letters* **76**, 3116 (1996).
- [12] D. L. Burke, R. C. Field, G. Horton-Smith, J. E. Spencer, D. Walz, S. C. Berridge, W. M. Bugg, K. Shmakov, A. W. Weidemann, C. Bula, K. T. McDonald, E. J. Prebys, C. Bamber, S. J. Boege, T. Koffas, T. Kotsieroglou, A. C. Melissinos, D. D. Meyerhofer, D. A. Reis, and W. Ragg, Positron production in multiphoton light-by-light scattering, *Physical Review Letters* **79**, 1626 (1997).
- [13] V. Yakimenko, L. Alsberg, E. Bong, G. Bouchard, C. Clarke, C. Emma, S. Green, C. Hast, M. J. Hogan, J. Seabury, N. Lipkowitz, B. O'Shea, D. Storey, G. White, and G. Yocky, FACET-II facility for advanced accelerator experimental tests, *Physical Review Accelerators and Beams* **22**, 101301 (2019).
- [14] H. Abramowicz, M. Altarelli, R. Aßmann, T. Behnke, Y. Benhammou, O. Borysov, M. Borysova, R. Brinkmann, F. Burkart, K. Büßer, O. Davidi, W. Decking, N. Elkina, H. Harsh, A. Hartin, I. Hartl, B. Heinemann, T. Heinzl, N. Tal Hod, M. Hoffmann, A. Ilderton, B. King, A. Levy, J. List, A. R. Maier, E. Negodin, G. Perez, I. Pomerantz, A. Ringwald, C. Rödel, M. Saimpert, F. Salgado, G. Sarri, I. Savoray, T. Teter, M. Wing, and M. Zepf, *Letter of intent for the LUXE experiment* (2019).
- [15] J. M. Cole, K. T. Behm, E. Gerstmayr, T. G. Blackburn, J. C. Wood, C. D. Baird, M. J. Duff, C. Harvey, A. Ilderton, A. S. Joglekar, K. Krushelnick, S. Kuschel, M. Marklund, P. McKenna, C. D. Murphy, K. Poder, C. P. Ridgers, G. M. Samarin, G. Sarri, D. R. Symes, A. G. Thomas, J. Warwick, M. Zepf, Z. Najmudin, and S. P. Mangles, Experimental Evidence of Radiation Reaction in the Collision of a High-Intensity Laser Pulse with a Laser-Wakefield Accelerated Electron Beam, *Physical Review X* **8**, 10.1103/PhysRevX.8.011020 (2018).
- [16] K. Poder, M. Tamburini, G. Sarri, A. Di Piazza, S. Kuschel, C. D. Baird, K. Behm, S. Bohlen, J. M. Cole, D. J. Corvan, M. Duff, E. Gerstmayr, C. H. Keitel, K. Krushelnick, S. P. Mangles, P. McKenna, C. D. Murphy, Z. Najmudin, C. P. Ridgers, G. M. Samarin, D. R. Symes, A. G. Thomas, J. Warwick, and M. Zepf, Experimental Signatures of the Quantum Nature of Radiation Reaction in the Field of an Ultraintense Laser, *Physical Review X* **8**, 31004 (2018).

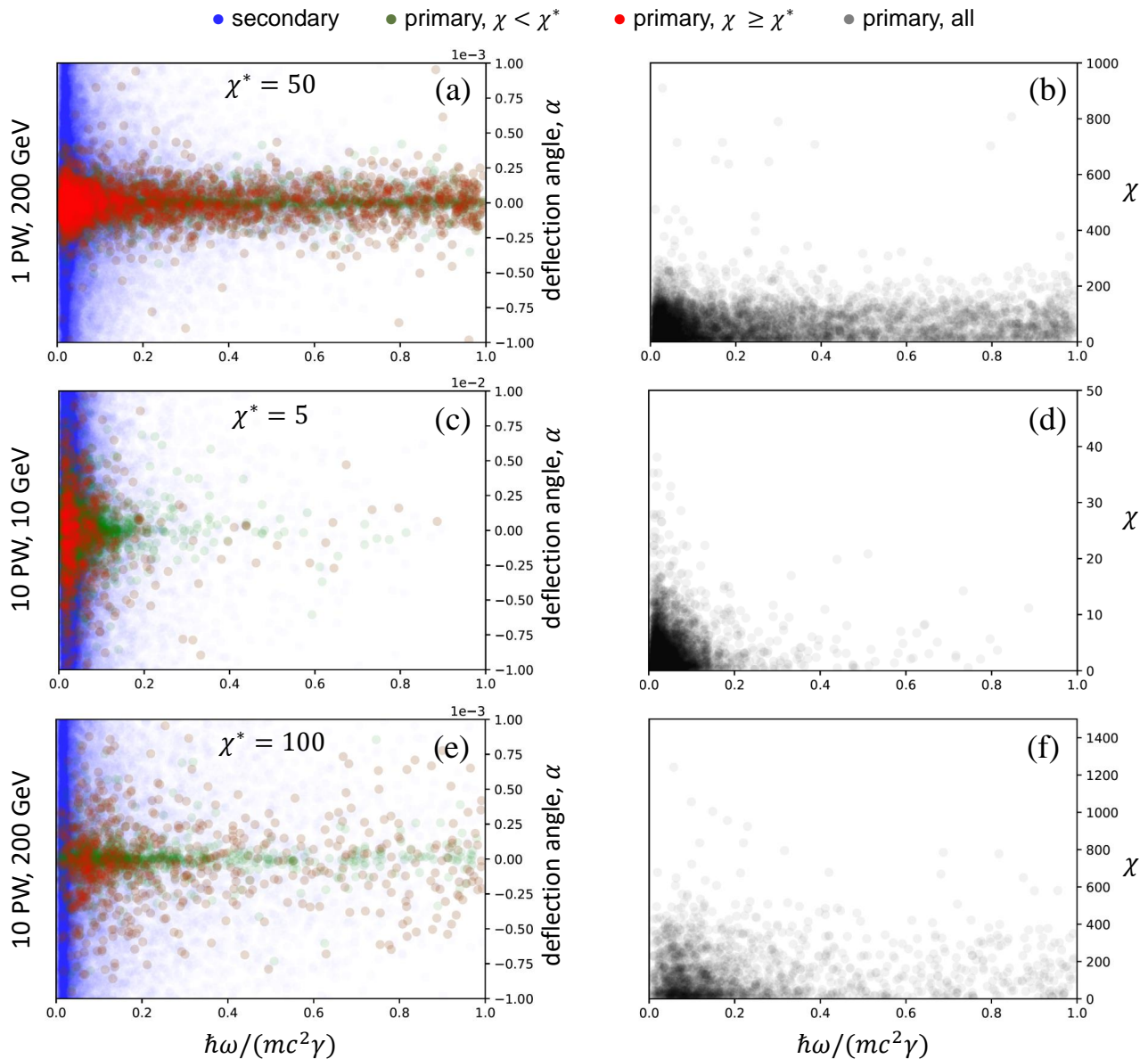


FIG. 3. The results of simulations for three experiments with laser power and electron energy shown on the left. The subplots show the distribution of photons via set of markers in the plane on normalized photon energy and the deflection angle α (a, c, e), as well as on the plane of normalized photon energy and the value of χ .

- [17] J. Magnusson, A. Gonoskov, M. Marklund, T. Esirkepov, J. Koga, K. Kondo, M. Kando, S. Bulanov, G. Korn, and S. Bulanov, Laser-particle collider for multi-GeV photon production, *Physical Review Letters* **122**, [10.1103/physrevlett.122.254801](https://doi.org/10.1103/physrevlett.122.254801) (2019).
- [18] I. M. Bassett, Limit to Concentration by Focusing, *Opt. Acta* **33**, 279 (1986).
- [19] I. Gonoskov, A. Aiello, S. Heugel, and G. Leuchs, Dipole pulse theory: Maximizing the field amplitude from 4π focused laser pulses, *Physical Review A - Atomic, Molecular, and Optical Physics* **86**, 053836 (2012).
- [20] S. S. Bulanov, V. D. Mur, N. B. Narozhny, J. Nees, and V. S. Popov, Multiple colliding electromagnetic pulses: A way to lower the threshold of e^+e^- pair production in vacuum, *Physical Review Letters* **104**, [10.1103/physrevlett.104.220404](https://doi.org/10.1103/physrevlett.104.220404) (2010).
- [21] A. Gonoskov, A. Bashinov, I. Gonoskov, C. Harvey, A. Ilderton, A. Kim, M. Marklund, G. Mourou, and A. Sergeev, Anomalous Radiative Trapping in Laser Fields of Extreme Intensity, *Physical Review Letters* **113**, 014801 (2014).
- [22] A. Gonoskov, A. Bashinov, S. Bastrakov, E. Efimenko, A. Ilderton, A. Kim, M. Marklund, I. Meyerov, A. Muraviev, and A. Sergeev, Ultrabright GeV photon source via controlled electromagnetic cascades in laser-dipole waves, *Physical Review X* **7**, 41003 (2017).
- [23] J. Magnusson, A. Gonoskov, M. Marklund, T. Z. Esirkepov, J. K. Koga, K. Kondo, M. Kando, S. V. Bulanov,

- G. Korn, C. G. Geddes, C. B. Schroeder, E. Esarey, and S. S. Bulanov, Multiple colliding laser pulses as a basis for studying high-field high-energy physics, *Physical Review A* **100**, [10.1103/PhysRevA.100.063404](#) (2019).
- [24] E. S. Efimenko, A. V. Bashinov, A. A. Gonoskov, S. I. Bastrakov, A. A. Muraviev, I. B. Meyerov, A. V. Kim, and A. M. Sergeev, Laser-driven plasma pinching in e-e+ cascade, *Physical Review E* **99**, [031201](#) (2019).
- [25] E. S. Efimenko, A. V. Bashinov, S. I. Bastrakov, A. A. Gonoskov, A. A. Muraviev, I. B. Meyerov, A. V. Kim, and A. M. Sergeev, Extreme plasma states in laser-governed vacuum breakdown, *Scientific Reports* **8**, [2329](#) (2018).
- [26] W. Panofsky, *Classical electricity and magnetism* (Dover Publications, Mineola, N.Y, 2005).
- [27] C. Sheppard and K. Larkin, Optimal concentration of electromagnetic radiation, *Journal of Modern Optics* **41**, [1495](#) (1994).